COBEM 2023 27TH INTERNATIONAL CONGRESS OF MECHANICAL ENGENEERING

ABCM Brazilian Society of Mechanical Sciences and Engineering
27th ABCM International Congress of Mechanical Engineering
December 04-08, 2023, Florianópolis-SC, Brazil

COB-2023-0715
COMPARISON OF DIFFERENT MATHEMATICAL MODELS FOR THE EVALUATION OF HEMOLYTIC AND TROMBOGENIC POTENTIALS IN CENTRAL VENOUS ACCESS FOR HEMODIALYSIS

Matheus Carvalho Barbosa Costa
Saulo de Freitas Gonçalves
Mário Luis Ferreira da Silva
Graduate Program in Mechanical Engineering – Universidade Federal de Minas Gerais, Avenida Antônio Carlos, 6627, Belo Horizonte, Minas Gerais, Brazil
mt94_carvalho@hotmail.com
saulodfg@gmail.com
marioluisfs@gmail.com

Thabata Coaglio Lucas
Universidade Federal dos Vales do Jequitinhonha e Mucuri, Rodovia MGT 367 – km 583, 5000, Diamantina, Minas Gerais, Brazil
thabataclucas@gmail.com

Rudolf Huebner
Universidade Federal de Minas Gerais, Avenida Antônio Carlos, 6627, Belo Horizonte, Minas Gerais, Brazil
rudolf@demec.ufmg.br

Abstract. *Central Venous Catheter is a form of vascular access to perform the hemodialysis procedure and is in increasing use worldwide. Despite the catheter has advantages over other forms of vascular access, it has some risks, such as thrombus formation and hemolysis. The present work aims to evaluate different mathematical models to estimate hemolytic and thrombogenic potentials in central venous access for hemodialysis using Computational Fluid Dynamics for different dialysis flow rates. The geometry of the central veins was obtained through a Computed Tomography of a healthy, male, 74-year-old patient and a MedCOMP/HEMO-CATH catheter model was used, with a dialysis flow rate of 0.0035 kg/s (200 mL/min), 0.0053 kg/s (300 mL/min) and 0.0071 kg/s (400 mL/min). The simulations were performed in a transient regime with physiological boundary conditions, using the k-ω SST turbulence model, the Carreau-Yasuda model for blood rheological behavior. Five Lagrangian and the Eulerian models were used to estimate the hemolytic and thrombogenic potentials. It is observed that the thrombogenic and hemolytic potentials increase due to the increase in the dialysis flow rate for all models. Furthermore, the models present different values, since the integrations along the trajectory lines are different for each model. With the present work, it can be observed that numerical studies are a viable alternative to study the possibility of improving hemodialysis procedures.*

Keywords: *Hemodialysis, Central Venous Catheter, Hemolytic Potential, Thrombogenic Potential, Computational Fluid Dynamics, Eulerian Model, Lagrangian Model.*

1. INTRODUCTION

Chronic Kidney Disease (CKD) is characterized by the reduced ability of the kidneys to perform their main functions, which are to remove of waste and excess water from the body. Among the available therapies that aim to partially replace kidney functions and relieve the symptoms of patients diagnosed with CKD, dialysis is a method of renal clearance that is in increasing use worldwide, with an estimated double of patients on dialysis in the year 2030 compared to the year 2010 (Chan et al., 2019, Zhao et al., 2021). Considering the total of this number, hemodialysis includes 89% of patients while peritoneal dialysis only 11% (Okpechi et al., 2022).

Central Venous Catheter (CVC) represents a vascular access for the hemodialysis procedure and is widely used, even though arteriovenous graft and arteriovenous fistula are the preferred methods to perform such access (de Oliveira et al., 2021, Owen et al., 2020, Park et al., 2020). Among the main advantages of the CVC, the relative ease of insertion, painless dialysis process and the possibility of immediate use can be highlighted (Gunawansa et al., 2018). However, catheters are also associated with risks of infections, increased thrombus formation and increased occurrence of hemolysis (Lucas et al., 2019). The increasing thrombus formation and the rupture of blood cells can cause obstructions in the CVC orifices, thus causing a decrease in the efficiency of the device over use time (Peng et al., 2017, Guilhermo-

Corpus et al., 2019), as well as increasing the incidence of other adversities, such as thrombosis, pulmonary embolism and reduced distribution of oxygen to tissues (Allon et al., 2017).

The processes of thrombus formation and hemolysis are associated with two parameters of blood flow that act together: shear stress and time of exposure to these stresses (Berg et al., 2019). This suggests that the dialysis flow rate during hemodialysis is an important factor for the efficiency of the procedure, since these quantities directly impact these two parameters (Costa et al., 2021). Thus, understanding the physical variables that govern the flow field that encompass the studied domain is fundamental for the complete analysis of these two mentioned phenomena.

A tool that appears as an alternative for the evaluation of hemodynamic factors that influence thrombus formation and hemolysis is the development of numerical models based on Computational Fluid Dynamics (CFD) (de Oliveira et al., 2021, Owen et al., 2020, Lucas et al., 2014). The main advantages of this tool are its relatively low cost and being non-invasive technique, with the possibility of inserting mathematical models to obtain hemolytic and thrombogenic potentials in the computational calculation process.

The mathematical models that aim to predict thrombus formation and hemolysis are divided into two groups: Lagrangian models and Eulerian models. To perform calculations using Lagrangian models, it is necessary to inject particles into the inlets of the computational domain, and the solutions depend on how the integration is carried out along the trajectory lines (Taskin et al., 2012). The Eulerian model, on the other hand, is based on partial differential equations, that is, this model presents a unique solution and is able to estimate the variables throughout the entire calculation domain (Taskin et al., 2012). However, there is still no consensus on which approach is more appropriate to quantify thrombus formation and hemolysis, due to the scarce existence of experimental evidence to compare with numerical results.

The present study aims to analyze, using the CFD technique, different mathematical models for the quantification of hemolytic potential and thrombogenic potential, for different dialysis flow rates, in central venous access for hemodialysis. In this way, we seek to contribute to the advancement of the CVC design, to reduce these complications that imply the removal and replacement of these devices from patients during the hemodialysis procedure, to guarantee a more efficient clinical process, and avoid risks related to the spread of other diseases resulting from these two phenomena.

2. MATERIALS AND METHODS

2.1 Geometry

The detailed process for obtaining the geometry of the central veins is described in Costa et al. (2022). The geometry was obtained through a computed tomography scan of a healthy, 74-year-old male patient. The procedure was approved by the Comitê de Ética em Pesquisa/Universidade Federal de Minas Gerais (CEP-UFMG) under the process number CAAE 02405712.5.1001.5149.

SolidWorks software (SolidWorks, Inc., Concord, MA, USA) was used to make a Computer Aided Design (CAD) of a MedCOMP/HEMO-CATH (Harleysville, PA, USA) clinical catheter model. This model is divided into an arterial lumen, where the patient's blood is guided to the dialyzer, and a venous lumen, where the blood returns to the patient. Figure 1a shows the geometry of the CVC, while Figure 1b shows the final geometry used in the simulations.

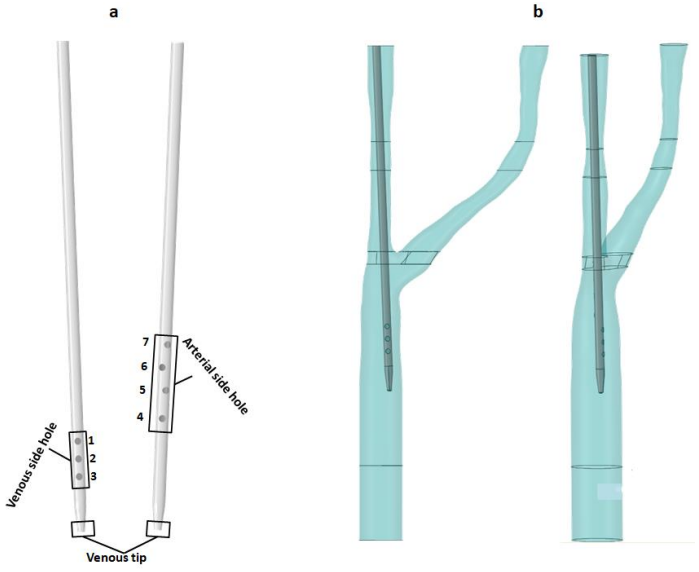

Figure 1. (a) Geometry of the CVC. (b) Final geometry used in the simulations.

2.2 PLI and HI mathematical models

The Lagragian and Eulerian mathematical models used to calculate the trombogenic potential and the hemolytic potential was based on the empirical model proposed by Giersiepen et al. (1990), Eq. (1).

$$PLI = HI = C_i t^{\alpha_i} \tau^{\beta_i}, \tag{1}$$

Taskin et al. (2012) described different Lagrangian models for calculating total thrombus formation and hemolysis, where all models are different ways of integrating the Eq. (1). The first model, indicated by Eq. (2), is based on temporal integration along a trajectory line of Eq. (1).

$$PLI1 = H1 = \sum C_i \Delta t^{\alpha_i} \tau^{\beta_i}, \tag{2}$$

This model fails to estimate the uniform shear stress and fails to reproduce the total thrombus formation and hemolysis given by Eq. (1). The next model was generated by integrating the time derivative of Eq. (1) and is represented by Eq. (3).

$$PLI2 = HI2 = \sum \alpha_i C_i t^{\alpha_i - 1} \tau^{\beta_i} \Delta t, \tag{3}$$

the main limitation of this model is that it does not incorporate the history of red cell damage, but this model can estimate the uniform shear stress field given by Eq. (1). The third method, Eq. (4), is based on the sum of damage linearized with respect to time.

$$PLI3 = HI3 = C_i \left[\sum \Delta t \tau^{\frac{\beta_i}{\alpha_i}} \right]^{\alpha_i}, \tag{4}$$

the main advantage of this model is the possibility of incorporating the damage history of cells. For the fourth Lagrangian model, Eq. (5), it is necessary to derive the mechanical dose D, Eq. (6), with respect to time.

$$PLI4 = HI4 = \sum \alpha_i C_i \left[\sum_{l=1}^{k} \tau(t_l)^{\frac{\beta_i}{\alpha_i}} \Delta t_l + D(t_0) \right]^{\alpha_i - 1} \tau(t)^{\frac{\beta_i}{\alpha_i}} \Delta t, \tag{5}$$

$$D = t\tau^{\frac{\beta_i}{\alpha_i}}, \tag{6}$$

where the term in the square brackets, in Eq. (5), represents the whole mechanical dose acting on the particle along the trajectory line from the starting observation time until the l-th instant. Finally, the last model considers that the contribution of damage at an instant of time is a function of the damage at that same instant, but it is independent of the way in which the damage occurred.

$$PLI5 = HI5 = C_i \left(t_{eff} + \Delta t \right)^{\alpha_i} \tau (t + \Delta t)^{\beta_i}, \tag{7}$$

$$t_{eff} = \left[\frac{PLI5(t)}{C_1 \tau (t+\Delta t)^{\beta_1}} \right]^{\frac{1}{\alpha_1}} or \left[\frac{HI5(t)}{C_2 \tau (t+\Delta t)^{\beta_2}} \right]^{\frac{1}{\alpha_2}}, \tag{8}$$

Lacasse et al. (2007) and Haniel et al. (2019) propose the following transport equation for calculating the trombogenic potential and hemolytic potential:

$$\frac{\partial PLI_L}{\partial t} + (\boldsymbol{u} \cdot \nabla) PLI_L = \delta C_1^{\frac{1}{\alpha_1}} \tau^{\frac{\beta_1}{\alpha_1}}, \tag{9}$$

$$\frac{\partial HI_L}{\partial t} + (\boldsymbol{u} \cdot \nabla) HI_L = \delta A \tau^{\frac{\alpha_2}{\beta_2}} (1 - HI_L), \tag{10}$$

where, τ is shear stress, t is exposure time, C_i, α_i and β_i are constants obtained through experimental data regression, $PLI_L = PLI^{\frac{1}{\beta_1}}$ and $HI_L = HI^{\frac{1}{\beta_2}}$ are the linear platelet lysis index and linear hemolysis index with respect to time (t), $\boldsymbol{u}$ is the velocity vector, $A = (C_2/100)^{\frac{1}{\beta_2}}$ and δ considers the limit value of shear stress (τ_s) required for platelet activation and hemolysis, given by:

$$\delta = \begin{cases} 0 \; if \; \tau < \tau_s \\ 1 \; if \; \tau \geq \tau_s \end{cases}, \tag{21}$$

wherein, the value generally used for τ_s is 10 Pa for PLI_L and 25 Pa for HI_L (Mareels et al., 2007, Lacasse et al., 2007). Table 1 show the values of C_i, α_i and β_i used in this work (Mareels et al., 2007, Giersiepen et al., 1990).

Table 1. Values of the empirical constants obtained through experimental data regression.

Empirical Parameter Values				
	i	**C**	**α**	**β**
PLI	1	3.66E-06	0.770	3.075
HI	2	3.62E-05	0.785	2.416

2.3 Numerical solution

Simulations to obtain blood flow parameters, as well as thrombogenic potential and hemolytic potential in the central venous access, were performed using the ANSYS-Fluent® 19.2 software (ANSYS-Fluent Inc., Lebanon, NH, USA).

The flow was considered incompressible and transient flow covering two complete cardiac cycles of 0.8 s, however, discarding the results of the first cycle. To model the turbulence, the k-ω SST (Shear Stress Transport) model was adopted, since this model combines the advantages of the k-ε model, which satisfactorily predicts the physical variables of the flow far from the boundary layer, and of the k–ω model, used for flows close to the boundary layer and when there are adverse pressure gradients. Regarding the characteristics of the blood, the value of 1060 kg/m^3 was used for the density, and for the rheological behavior the Carreau-Yasuda model, Eq. (12), was adopted with the following values for the parameters: Minimum Viscosity $(\eta_0) = 0.0035$ kg/s, Maximum Viscosity $(\eta_\infty) = 0.056$ kg/s, Power Law Index$(n) = 0.3568$ and Time Constant $(\lambda) = 3.313$ s (Kumar et al., 2019, Costa et al., 2021).

$$\frac{\eta - \eta_\infty}{\eta_0 - \eta_\infty} = \left[1 + \left(\lambda \dot{\gamma}_{xy}\right)^a\right]^{\frac{n-1}{a}}, \tag{32}$$

A time step of 2x10^{-3} s was adopted, thus totaling 400 time steps for each complete cardiac cycle of 0.8 s, to guarantee a Courant number close to unity, as recommended by the Courant-Friedrichs-Lewis Condition.

The coupled algorithm was used for the Pressure-Velocity coupling. The second order upwind method was used for the spatial discretization of the momentum equation, turbulent kinetic energy and specific rate of dissipation. The PRESTO! was used for the pressure interpolation. The implicit second-order scheme was adopted for the temporal discretization. The Least Squares Cell-Based method was used for the discretization of the gradient terms. The first-order upwind method was adopted for the discretization of the PLI_L and HI_L models. In ANSYS-Fluent the continuity discretization is based on the method presented by Rhie and Chow (1983). A convergence criterion of 10^{-4} was considered for the numerical residual for all variables.

The models to calculate the HI_L and PLI_L were added to the ANSYS-Fluent® 19.2 software solver. The initial condition for the quantities HI_L and PLI_L was considered zero. Finally, to perform the post-processing of the Lagrangian models, it was necessary to release particles in the computational domain inlets to map the trajectory lines, and the integrations and calculations of the averages in relation to the trajectory lines were carried out in the MatlabMathworks® software.

2.4 Boundary Conditions

The physiological boundary conditions used in this work were obtained from the flow rate curves in the superior vena cava and the pressure of the right atrium in the studies of Markl et al. (2011) and Mynard and Smolich (2015). The flow rates at the inlets of the right and left jugular veins were considered equal to half of the total flow rate of the superior vena cava, and this is justified by the scarcity of data in the literature and the absence of consensus on the values of the flow rates in the right and left jugular veins. However, it was decided to use velocities at the inlets of the jugular veins, as the flow rate made the convergence process difficult. Figure 2 shows the curves for the two variables used in the boundary conditions.

In order to assess the impacts on the hemolytic and thrombogenic potentials fields due to changes in dialysis flow rates, three different flow rates at the catheter inlet were considered: 0.0035 kg/s (200 mL/min), 0.0053 kg/s (300 mL/min) and 0.0071 kg/s (400 mL/min) (Kousoula et al., 2019, Besarab and Pandey, 2011, Petridis et al., 2017).

A non-slip condition was adopted for the walls of the veins and the CVC. For HI_L and PLI_L, a zero value was applied to the domain inlets, $HI_L = PLI_L = 0$, and zero flux on the walls and at the outlet of the computational domain, $\frac{\partial HI_L}{\partial n} = \frac{\partial PLI_L}{\partial n} = 0$.

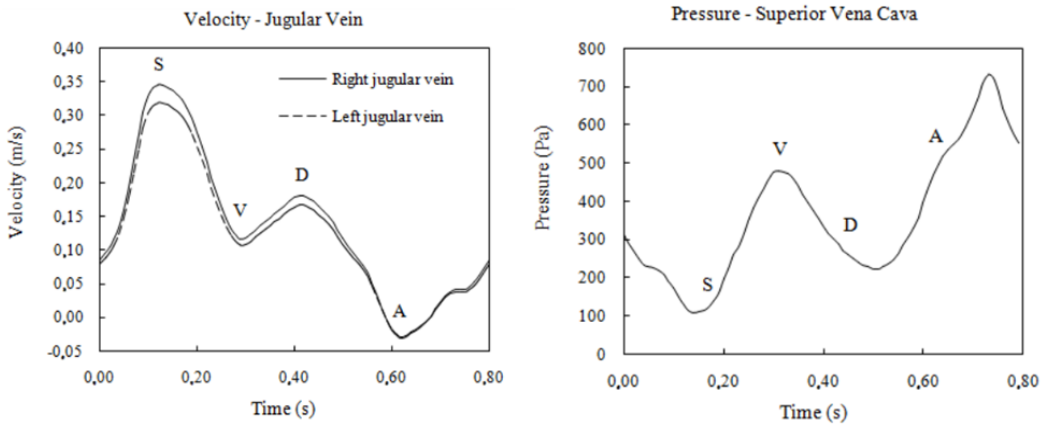

Figure 2. Velocity inlets and pressure outlet curves in the central veins. The instants of the cardiac cycle that occur to atrial contraction (A), systole (S), transitional wave (V) and diastole (D) are indicate.

For the calculation of Lagrangian models, the injected particles were allowed to escape at the inlets and outlets of the geometry and reflect on the walls of the veins and the catheter.

2.5 Mesh convergence tests

For the mesh convergence analysis, the pressure and velocity results were monitored in four planes close to the tip and lateral orifices of the catheter, since these are regions with greater gradients for these variables. The meshes were refined by doubling the number of elements, which resulted in the grid refinement factor, Eq. (13), close to 1.3, as recommended by the ASME V & V 20 standard.

$$r_{ij} = \frac{h_i}{h_j}, \tag{43}$$

where, h_i is the characteristic length of the course grid and h_j is the characteristic length of the fine mesh. The characteristic length was calculated by the Eq. (14).

$$h = \left[\frac{1}{N}\sum_{i=1}^{N} \Delta V_i\right]^{\frac{1}{3}}, \tag{54}$$

where, ΔV_i is the volume of the i-th element and N is the total number of the elements.

The grids were refined until the differences in the mean values of pressure and velocity in the defined planes were close to 5%. Table 2 shows the characteristics of the tested meshes and the relative errors in the four analyzed planes.

Table 2. Characteristics of the tested meshes and the relative errors in the four analyzed planes.

Meshes			
	Mesh 1	**Mesh 2**	**Mesh 3**
# Elements	839864	1651824	3648883
# Nodes	286231	552404	1226046
Relative Error: Velocity			
Plane	**Mesh 2 – Mesh 1**		**Mesh 3 – Mesh 2**
Venous orifice 1 (%)	3.34		1.83
Venous orifice 2 (%)	1.92		3.93
Arterial orifice 4 (%)	1.79		5.52
Close to venous tip (%)	3.83		3.11
Relative Error: Pressure			
Plane	**Mesh 2 – Mesh 1**		**Mesh 3 – Mesh 2**
Venous orifice 1 (%)	0.58		0.69
Venous orifice 2 (%)	1.28		0.92
Arterial orifice 4 (%)	1.64		1.10
Close to venous tip (%)	0.52		0.39

To perform the simulations, mesh 2 was selected, as this mesh obeys the criterion of the difference being less than 5% for the variables analyzed and the numerical residual reaching a value lower than 10^{-4}.

3. RESULTS AND DISCUSSION

Figure 3 presents a comparison between iso-volumes of the linear platelet lysis index and the linear hemolysis index evaluated for the instant of maximum velocity of the cardiac cycle (t = 0.14 s) for each flow rate passing inside the catheter.

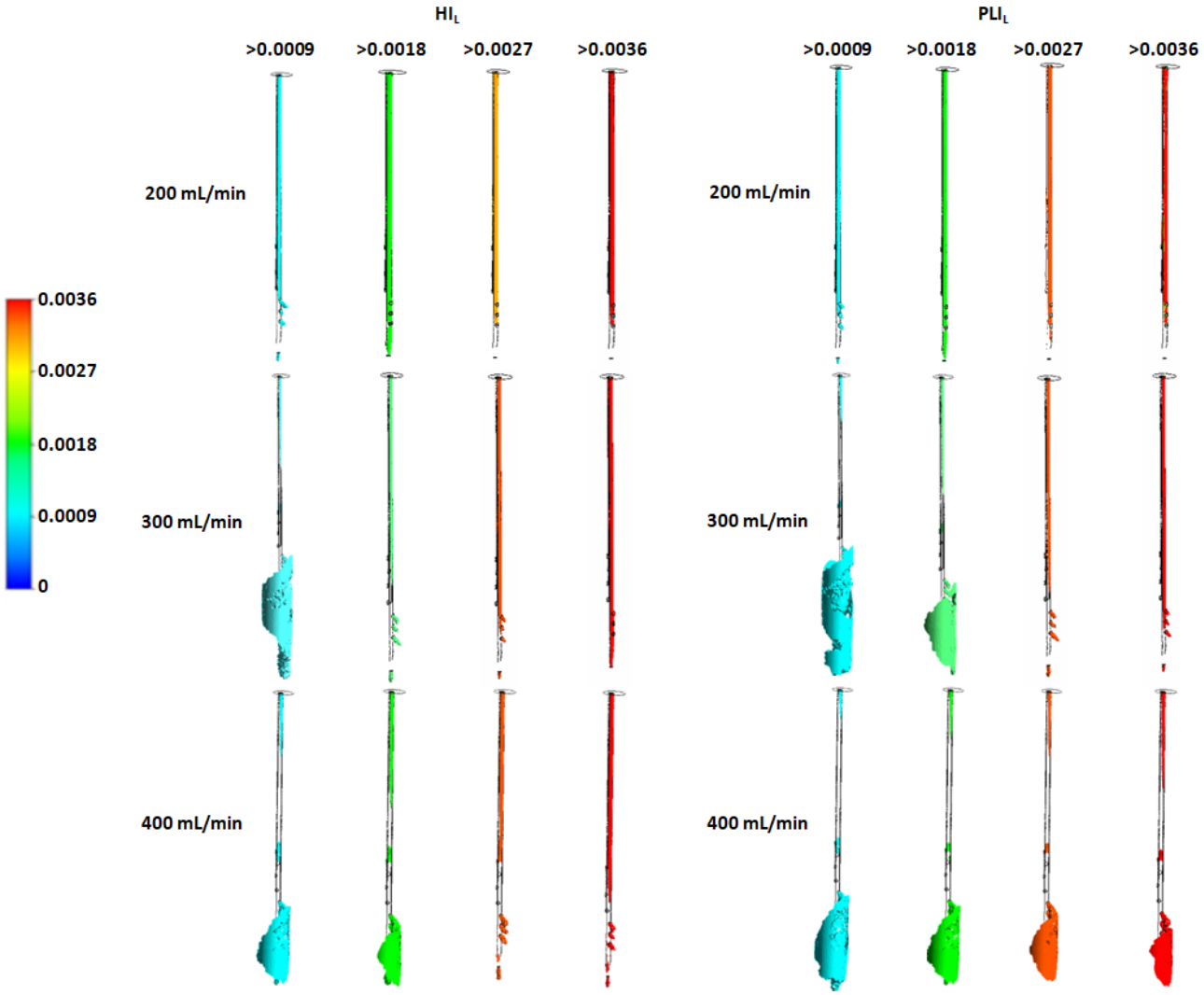

Figure 3. Iso-volumes of PLIL e HIL for each dialysis flow rate for instant of maximum velocity of cardiac cycle.

Higher flow rates in the catheter generated higher PLI_L and HI_L, mainly near the tip and venous orifices of the CVC. For a flow rate of 400 mL/min, the extension of the iso-volumes of PLI_L and HI_L representing values above 0.0027 and 0.0036 are greater in relation to the other dialysis flow rates. This can be explained, since, for higher dialysis flow rate, there is a tendency to increase shear stresses in regions close to the tip and venous orifices of the CVC (Gonçalves et al., 2020). Nevertheless, the flow rate of 300 mL/min showed greater extensions of iso-volumes for values above 0.0009 for PLI_L and HI_L. This may be related to the larger recirculation zones around the CVC outlets for this dialysis flow rate (Lucas et al., 2014), which are responsible for the increase in exposure time in these regions. Furthermore, it is observed that the extensions of iso-volumes for PLI_L were greater than for HI_L, thus indicating that thrombus formation is more critical than hemolysis in the case studied.

100 particles were selected to that enter the numerical domain through the CVC inlet to make the comparison between the Lagragian and Eulerian models. Figure 4 and Figure 5 show the PLI and HI values for the different mathematical models in relation to the dialysis flow rate.

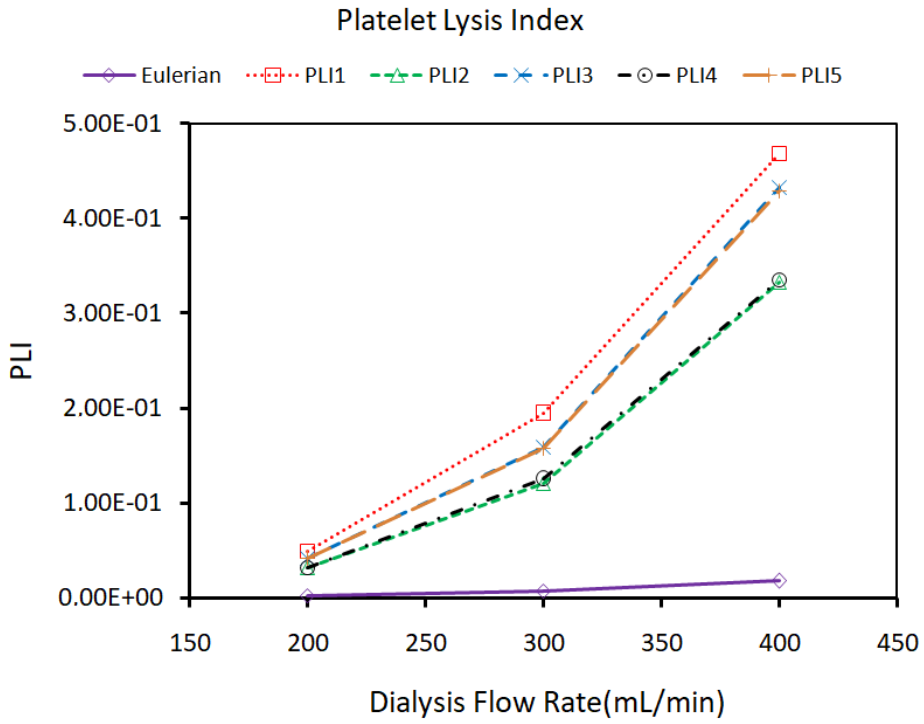

Figure 4. PLI values for the different mathematical models in relation to the dialysis flow rate.

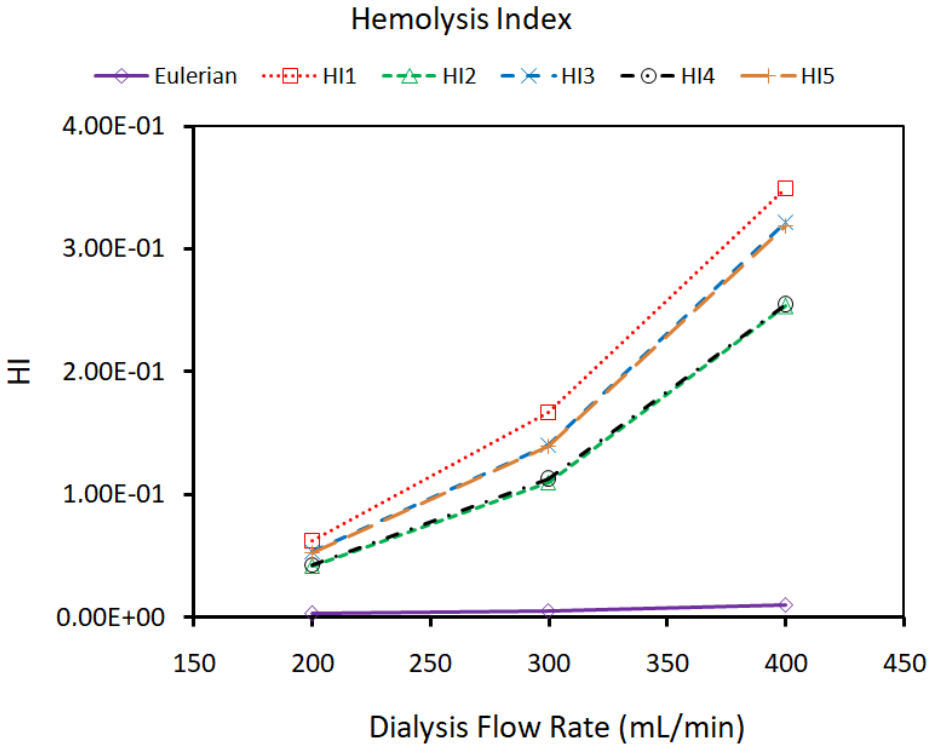

Figure 5. HI values for the different mathematical models in relation to the dialysis flow rate.

First, it is possible to observe that, for all models, the hemolysis index and the platelet lysis index increased due to the increase in the dialysis flow rate. This fact was previously observed only for the Eulerian model, and this increase in PLI and HI is caused by the significant increase in shear stress in the region close to the venous orifices of the CVC. These patterns were also observed by Haniel et al. (2021).

It is also observed that the results found for the Eulerian model are underestimated in comparison with the Lagrangian models, approximately 10 times smaller. This indicates that the Eulerian model is not capable of predicting

the true value of these two variables, and can therefore only be used for qualitative analyses or for observing PLI and HI patterns. Furthermore, the first Lagrangian model (HI1 and PLI1) presented the highest values, that is, the results were overestimated. It should be noted that this model is characterized by failing to estimate a uniform shear stress, as described in Eq. (1), and does not reproduce hemolysis and thrombus formation precisely (Taskin et al., 2012).

The second Lagrangian model (HI2 and PLI2) is characterized by lower values of PLI and HI among the Lagrangian models. This occurs because it has the limitation of not incorporating the history of red blood cell damage. Furthermore, it can be observed that the second and fourth (HI4 and PLI4) Lagrangian models presented similar results, however, the fourth model was subtly higher, since this model takes into account the history of blood cell damage. The third model (HI3 and PLI3) and the fifth model (HI5 and PLI5) presented intermediate results among the Lagrangian models. However, in other studies, the third and fourth models showed similar results, since they have the same characteristic of considering the history of particle damage (Taskin et al., 2012, Ho et al., 2020), and this was not observed for the system studied here.

Finally, the differences between the Lagrangian models increase with the growth of the dialysis flow rate, that is, for lower dialysis flow rates, the results for the five Lagrangian models were similar. This suggests that there is the possibility of using simpler models to estimate thrombus formation and hemolysis for the hemodialysis procedure with low flow rates. It should be highlighted that the work has the limitation of not having experimental data to compare with numerical data, and it is not known which model is more indicated.

4. CONCLUSION

Numerical models based on computational fluid dynamics allow the investigation of hemodynamic parameters that can influence thrombus formation and hemolysis in a non-invasive way and relatively low cost.This tool can be used to assist healthcare professionals, so that clinical procedures are performed more efficiently, ensuring comfort for the patient.

Controlling of dialysis flow is a crucial factor for hemodialysis, as this variable is closely related to the patient's dialysis time. In this case, as the dialysis flow rate increases, the time to complete the procedure will decrease. However, it is noticed that the platelet lysis index and the hemolysis index increase significantly with the increase in the dialysis flow rate. Therefore, it is necessary to make an adequate choice of flow, so that the dialysis time is not high and that the formation of thrombi and hemolysis is not so detrimental for the patient and the efficiency of the clinical process.

Finally, the differences between the Lagrangian models increase with the growth of the dialysis flow rate, that is, for lower dialysis flow rates the results for the four Lagrangian models were similar. This suggests that, for low flow rates, there is the possibility of using simpler models to estimate thrombus formation and hemolysis for the hemodialysis procedure. In addition, the Eulerian model, compared to the Lagrangian models, presented underestimated results, that is, it was only qualitatively valid.

5. REFERENCES

Allon, M., Brouwer-Maier, D.J., Kenneth, B., et al., 2017. Recommended Clinical Trial End Points for Dialysis Catheters.*Clinical Journal of the American Society of Nephrology*, Vol. 12, pp. 495-500.

Berg, N., Fuchs, L., Prahl, W.L., 2019. Flow Characteristics and Coherent Structures in a Centrifugal Blood Pump.*Flow, Turbulence and Combustion*, Vol. 102, pp. 469-483.

Besarab, A., and Pandey, R., 2011. Catheter management in hemodialysis patients: Delivering adequate flow. *Clinical Journal of the American Society of Nephrology*, Vol. 6, pp. 227-234.

Chan, C.T., Blankestijn, P.J., Dember, L.M., et al., 2019. Dialysis initiation, modality choice, access, and prescription: conclusions from a Kidney Disease. *Kidney International*, Vol. 96, pp. 37-47.

Costa, M.C.B, Gonçalves, S.D.F., Lucas, T.C., et al., 2022. Development of a Non-Rigid Model Representing the Venous System of a Specific Patient. *Springer XXVII Brazilian Congress on Biomedical Engineering*, Vol. 83.

Costa, M.C.B., Gonçalves, S.D.F., Silva, M.L.F., Lucas, T.C., Huebner, R., 2021. Evaluation of Hemolytic Potentials by Eulerian Approach in Central Venous Access for Hemodialysis. In *Proceeding of the 26th International Congress of Mechanical Engineering* – COBEM 2021. Virtual Congress, Brazil.

De Oliveira, D.C., Owen, D.G., Qian, S., Green, N.C., Espino, D.M., and Shepherd, D.E.T., 2021. Computational fluid dynamics of the right atrium: Assessment of modelling criteria for the evaluation of dialysis catheters. *PLoS One*, Vol. 16(2).

Giersiepen, M., Wurzinger, L.J., Opitz, R., and Reul, H., 1990. Estimation of Shear Stress-Related Blood Damage in Heart Valve Prostheses – In Vitro Comparison of 25 Aortic Valve. *The International Journal of Artificial Organs*, Vol. 13, pp. 300-306.

Gonçalves, S.F., Costa, M.C.B., Lucas, T.C., et al., 2020. Evaluation of different turbulence models for the characterization of shear stresses in the central venous access for hemodialysis. In *Proceeding of the 18th Brazilian Congress of Thermal Sciences and Engineering* – ENCIT 2020, Virtual Congress, Brazil.

Gunawansa, N., Sudusinghe, D.H., and Wijayaratne, D.R., 2018. Hemodialysis Catheter-Related Central Venous Thrombosis: Clinical Approach to Evaluation and Management. *Annals of Vascular Surgery*, Vol. 51, pp. 298-305.

Guilermo-Corpus, G., Ramos-Gordillo, J.M., Peña-Rodriguez, J.C., 2019. Survival and Clinical Outcomes of Tunneled Central Jugular and Femoral Catheters in Prevalent Hemodialysis Patients. *Blood Purification*, Vol. 47, pp. 132-139.

Haniel, J., Lucas, T.C., and Huebner, R., 2019. Evaluation of Thrombogenic Potential by Partial Diferential Equations in the Blood Flow Dynamics With Central Venous Catheter. *Journal of the Brazilian Society of Mechanical Sciences and Engineering*, 41, 299.

Haniel, J., Lucas, T.C., Silva, M.L.F., Gomes, V.S., and Huebner, R., 2021. Influence of hemodialysis blood flow rate on the thrombogenic potential in patients with central venous catheters. *Anais da Academia Brasileira de Ciências*, Vol. 93(3).

Ho, M.G.C. et al., 2020. Comparative Study Between Eulerian and Lagragian Approaches for the Analysis of Hemolytic and Platelet Lysis Index With Couette Flow. In *Proceeding of the 18th Brazilian Congress of Thermal Sciences and Engineering*. November 16-20, 2020.

Kousoula, V., Georgianos, P.I., Mavromatidis, K., et al., 2019. Reversed connection of cuffed, tunneled, dual-lumen catheters with increased blood flow rate maintains the adequacy of delivered dialysis despite the higher access recirculation. *International Urology and Nephrology*, Vol. 51, pp. 1841-1847.

Kumar, N., Khader, A., Pai, R., Kyriacou, P., Khan, S., and Koteshwara, P., 2019. Computational fluid dynamic study on effect of Carreau: Yasuda and Newtonian blood viscosity models on hemodynamic parameters. *Journal of Computational Methods in Sciences and Engineering*, Vo.l.19, pp.465-477.

Lacasse, D.,Garon, A. and Pelletier, D., 2007. Mechanical Hemolysis in Blood Flow: User-Independent predictions with the Solution of a Partial Differential Equation. *Computer Methods in Biomechanics and Biomedical Engineering*, Vol. 10, No. 1, pp. 1-12.

Lucas, T.C., Tessarolo, F., Jakitsch, V., Caola, I., Brunori, G., Nollo, G., and Huebner, R., 2014. Blood Flow in Hemodialysis Catheters: A Numerical Simulation and Microscopic Analysis of In Vivo-Formed Fibrin. *Artificial Organs*, Vol. 38, pp. 556-565.

Lucas, T.C., Haniel, J., Huebner, R., 2019. Numerical simulation of blood fluid in hemodialysis catheters and its thrombogenic potential. *ActaScientiarum – Health Sciences*, Vol. 41

Mareels, G., Kaminsky, R., Eloot, S., Verdonck, P.R., 2007. Particle Image Velocimetry-Validated, Computational Fluid Dynamics-Based Design to Reduce Shear Stress and Residence Time in Central Venous Hemodialysis Catheters. *Journal ASAIO*, Vol. 53, 4th edition, pp. 438-446.

Markl, M. et al., 2011. Time-resolved three-dimensional magnetic resonance velocity mapping of cardiovascular flow paths in volunteers and patients with Fontan circulation. *European Journal of Cardio-thoracic Surgery*, Vol. 39, No. 2, pp. 206–212.

Mynard, J. O. P. M., and Smolich, J. O. J. S., 2015. One-Dimensional Haemodynamic Modeling and Wave Dynamics in the Entire Adult Circulation. *Annals of Biomedical Engineering*, Vol. 43, No. 6, pp. 1443– 1460.

Okpechi, I.G., Jha, V., Cho, Y., et al., 2022. The case for increased peritoneal dialysis utilization in low-and lower-middle-income countries. *Nephrology*, Vol. 27, pp. 391-403.

Owen, D.G., De Oliveira, D.C., Qian, S., Green, N.C., Shepherd, D.E.T., and Espino, D.M., 2020. Impact of side-hole geometry on the performance of hemodialysis catheter tips: A computational fluid dynamics assessment. *PLoS One*, Vol. 15(8).

Park, M.H., Qiu, Y., Cao, H., Yuan, D., Li, D., Jiang, Y., Peng, L. and Zheng, T., 2020. Influence of Hemodialysis Catheter Insertion on Hemodynamics in the Central Veins. *Journal of Biomechanical Engineering*, Vol. 142(9).

Peng, L., Qiu, Y., Huang, Z., Xia, C., Dai, C., Zheng, T., Li, Z., 2017. Numerical Simulation of Hemodynamic Changes in Central Veins after Tunneled Cuffed Central Venous Catheter Placement in Patients under Hemodialysis. *Scientific Reports*, Vol. 7, pp. 1-8.

Petridis, C., Nitschke, M., Lehne, W., et al., 2017. Tip Design of Hemodialysis Catheters Influences Thrombotic Events and Replacement Rate. *European Journal of Vascular and Endovascular Surgery*, Vol. 53, pp. 262-267.

Taskin, M.E., Fraser, K.H., Zhang, T., Wu, C., Griffith, B.P., and Wu, Z.J., 2012. Evaluation of Eulerian and Lagragian Models for hemolysis Estimation. *ASAIO Journal*, Vol. 58, pp. 363-372.

The American society of mechanical engineers, Standard for verification and validation in computational fluid dynamics and heat transfer – asme v&v 20-2009, Norma, The American Society of Mechanical Engineers (November 2009).

Zhao, X., Qingyu, N., Gan, L., et al., 2021. Baseline data report of the China Dialysis Outcomes and Practice Patterns Study (DOPPS). *Scientific Reports*, Vol. 11, n. 873.

6. RESPONSIBILITY NOTICE

The authors are the only responsible for the printed material included in this paper.